



Article scientifique

Article

2006

Published version

Open Access

This is the published version of the publication, made available in accordance with the publisher's policy.

[CpNi(dithiolene)] (and Diselenolene) Neutral Radical Complexes

Nomura, Mitsushiro; Cauchy, Thomas; Geoffroy, Michel; Adkine, Prashant Madhukar; Fourmigué, Marc

How to cite

NOMURA, Mitsushiro et al. [CpNi(dithiolene)] (and Diselenolene) Neutral Radical Complexes. In: Inorganic chemistry, 2006, vol. 45, n° 20, p. 8194–8204. doi: 10.1021/ic0608546

This publication URL: <https://archive-ouverte.unige.ch/unige:3639>

Publication DOI: [10.1021/ic0608546](https://doi.org/10.1021/ic0608546)

[CpNi(dithiolene)] (and Diselenolene) Neutral Radical Complexes

Mitsushiro Nomura,^{†‡} Thomas Cauchy,^{†§} Michel Geoffroy,^{||} Prashant Adkine,^{||} and Marc Fourmigué^{*†‡}

Laboratoire "Chimie, Ingénierie Moléculaire et Matériaux d'Angers" (CIMMA), UMR 6200 CNRS, Université d'Angers, UFR Sciences, Bât. K, 2 Bd. Lavoisier, 49045 Angers, France, Sciences Chimiques de Rennes, UMR 6226 CNRS, Université Rennes I, Campus de Beaulieu, 35042 Rennes Cedex, France, Department de Química Inorganica, Universitat de Barcelona, Diagonal 647, 08028 Barcelona, Spain, and Department of Physical Chemistry, University of Geneva, 30 Quai Ernest Ansermet, 1211, Geneva, Switzerland

Received May 17, 2006

Various preparations of the neutral radical [CpNi(ddd)] complex (ddd = 5,6-dihydro-1,4-dithiin-2,3-dithiolate) were investigated with CpNi sources, [Cp₂Ni], [Cp₂Ni](BF₄), [CpNi(CO)]₂, and [CpNi(cod)](BF₄), and dithiolene transfer sources, O=C(ddd), the naked dithiolate (ddd²⁻), the monoanion of square-planar Ni dithiolene complex (NBu₄)-[Ni(ddd)₂], and the neutral complex [Ni(ddd)₂]. The reaction of [CpNi(cod)](BF₄) with (NBu₄)[Ni(ddd)₂] gave the highest yield for the preparation of [CpNi(ddd)] (86%). [CpNi(ddds)] (ddds = 5,6-dihydro-1,4-dithiin-2,3-diselenolate), [CpNi(dsdt)] (dsdt = 5,6-dihydro-1,4-diselenin-2,3-dithiolate), [CpNi(bdt)] (bdt = 1,2-benzenedithiolate), and [CpNi(bds)] (bds = 1,2-benzenediselenolate) were synthesized by the reactions of [Cp₂Ni] with the corresponding neutral Ni dithiolene complexes [Ni(ddds)₂], [Ni(dsdt)₂], [Ni(bdt)₂], and [Ni(bds)₂], respectively. The five, formally Ni^{III}, radical complexes oxidize and reduce reversibly. They exhibit, in the neutral state, a strong absorption in the NIR region, from 1000 nm in the dddt/ddds/dsdt series to 720 nm in the bdt/bds series with ϵ values between 2500 and 5000 M⁻¹ cm⁻¹. The molecular and solid state structures of the five complexes were determined by X-ray structure analyses. [CpNi(ddd)] and [CpNi(ddds)] are isostructural, while [CpNi(dsdt)] exhibits a closely related structure. Similarly, [CpNi(bdt)] and [CpNi(bds)] are also isostructural. Correlations between structural data and magnetic measurements show the presence of alternated spin chains in [CpNi(ddd)], [CpNi(ddds)], and [CpNi(dsdt)], while a remarkably strong antiferromagnetic interaction in [CpNi(bdt)] and [CpNi(bds)] is attributed to a Cp...Cp face-to-face σ overlap, an original feature in organometallic radical complexes.

Introduction

Dithiolene complexes with a central Ni atom are the most investigated of the metal dithiolene complexes. Since the first square-planar Ni bis(dithiolene) complex reported in 1960,¹ Ni dithiolene complexes have been thoroughly investigated from the viewpoint of optical,² magnetic,³ and conductive studies.⁴ Most of these Ni dithiolene complexes are of the square-planar type,⁵ and they are well-known to exist in

several well-defined oxidation states.⁶ Heteroleptic complexes associating dithiolate and cyclopentadienyl ligands have been much less investigated. Such Cp–metal–dithiolene complexes can be classified into four main categories:⁷ the 2:2 Cp/dithiolene complexes formulated as [CpM(dithiolene)]₂ (M = group 5, 6, and 8 metals), the 2:1 Cp/dithiolene complexes [Cp₂M(dithiolene)] (M = group 4–6 metals), the

* To whom correspondence should be addressed. E-mail: marc.fourmigue@univ-rennes1.fr.

[†] Université d'Angers.

[‡] Université Rennes I.

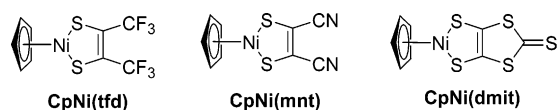
[§] Universitat de Barcelona.

^{||} University of Geneva.

- (1) (a) Schrauzer, G. N.; Meyweg, V. P. *J. Am. Chem. Soc.* **1962**, *84*, 3221. (b) Davison, A.; Edelstein, N.; Holm, R. H.; Maki, A. H. *J. Am. Chem. Soc.* **1963**, *85*, 2029. (c) Schrauzer, G. N.; Meyweg, V. P. *J. Am. Chem. Soc.* **1965**, *87*, 1483.
(2) (a) Cummings, S. D.; Eisenberg, R. *Prog. Inorg. Chem.* **2003**, *52*, 315. (b) Kisch, H. *Coord. Chem. Rev.* **1993**, *125*, 155.

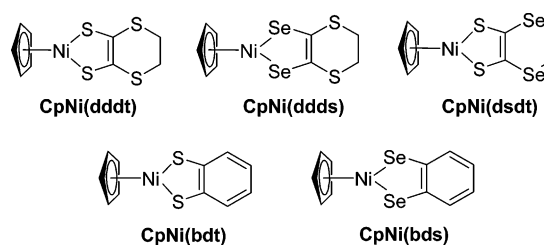
- (3) (a) Fourmigué, M. *Acc. Chem. Res.* **2004**, *37*, 179. (b) Coomber, A. T.; Beljonne, D.; Friend, R. H.; Bredas, J. L.; Charlton, A.; Robertson, N.; Underhill, A. E.; Kurmoo, M.; Day, P. *Nature* **1996**, *380*, 144. (c) Faulmann, C.; Cassoux, P. *Prog. Inorg. Chem.* **2003**, *52*, 399.
(4) (a) Cassoux, P.; Valade, L.; Kobayashi, H.; Kobayashi, A.; Clark, R. A.; Underhill, A. E. *Coord. Chem. Rev.* **1991**, *110*, 115. (b) Olk, R.-M.; Olk, B.; Dietzsch, W.; Kirmse, R.; Hoyer, E. *Coord. Chem. Rev.* **1992**, *117*, 99. (c) Kato, R. *Chem. Rev.* **2004**, *104*, 5319. (d) Matsubayashi, G.; Nakano, M.; Tamura, H. *Coord. Chem. Rev.* **2002**, *226*, 143.
(5) Beswick, C. L.; Schulman, J. M.; Stiefel, E. I. *Prog. Inorg. Chem.* **2003**, *52*, 55.
(6) Wang, K. *Prog. Inorg. Chem.* **2003**, *52*, 267.
(7) Fourmigué, M. *Coord. Chem. Rev.* **1998**, *178*, 823 and references therein.

Chart 1

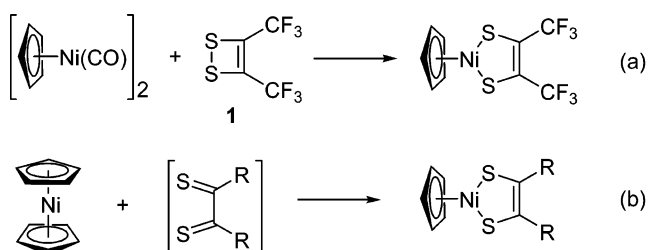


1:2 Cp/dithiolene complexes [CpM(dithiolene)₂] (M = group 4–7 metals), and the 1:1 Cp/dithiolene complexes [CpM(dithiolene)] (M = group 9 and 10 metals). The CpNi dithiolene complexes are included into the fourth category but are quite rare. King first reported the synthesis of [CpNi(tfd)] (tfd = 1,2-bis(trifluoromethyl)dithiolate, Cp = η^5 -cyclopentadienyl),⁸ and Wharton reported the η^4 -cyclobutadiene Ni dithiolene complex which is formulated as $[(\eta^4\text{-C}_4\text{R}_4)\text{Ni}(\text{mnt})]$ (mnt = maleonitriledithiolate).⁹ More recently, Faulmann et al. synthesized [CpNi(dmit)] (dmit = 1,3-dithiol-2-thione-4,5-dithiolate) serendipitously from the reaction of [Cp₂Ni](BF₄) with Na[Ni(dmit)₂]. The expected salt [Cp₂Ni][Ni(dmit)₂] was not obtained but rather the neutral paramagnetic complex [CpNi(dmit)].¹⁰ We have recently started a thorough investigation of the chemistry of the CpNi dithiolene complexes,^{11,12} for the following attractive reasons: (1) their synthetic methods are unique (Schemes 1–3) and provide new organometallic reactions; (2) these complexes are paramagnetic in the neutral state (formally Ni^{III}), hence strong magnetic interactions in the crystalline solid state can be anticipated from the absence of any counterion;¹¹ (3) these complex are quite soluble in organic solvents thanks to the Cp ligand, and single crystals are easily obtained by recrystallization^{11,12} without need for electrocrystallization experiments;¹³ and (4) some of these complexes exhibit an electronic absorption in the near-IR region,¹² an original feature also observed in the square-planar Ni dithiolene complexes.¹⁴ Therefore, the CpNi(dithiolene) complexes are very attractive from the organometallic, magnetic, and optical points of view. We report here a comparative investigation of different synthetic methods for the preparation of such complexes based on the novel complex [CpNi(dddt)] (dddt = 5,6-dihydro-1,4-dithiin-2,3-dithiolate) and describe the preparation of the selenium-containing analogues CpNi(ddds) and CpNi(dsdt), together with similar complexes based on benzenedithiol (i.e., CpNi(bdt) and CpNi(bds)). The X-ray crystal structures and electrochemical and magnetic properties of the five novel CpNi dithiolene complexes have been investigated in detail with special emphasis on (i) a NIR absorption band observed in all complexes but at different energies and (ii) the antiferromagnetic interactions present in the crystalline phases, as reflected by the analysis of the temperature dependence of the magnetic susceptibility.

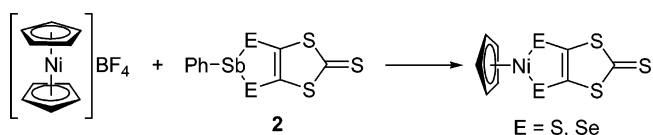
Chart 2



Scheme 1



Scheme 2



Results and Discussion

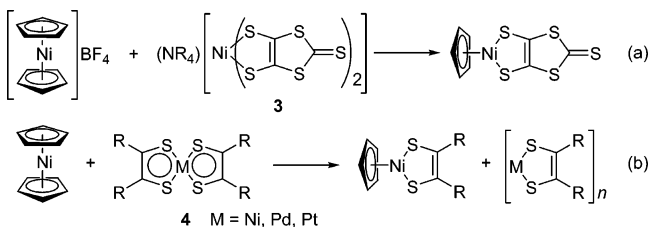
Syntheses of CpNi Dithiolene and Diselenolene Complexes. The described syntheses of these formally Ni^{III} CpNi dithiolene complexes involve a CpNi source and a dithiolene transfer source, together with an appropriate redox match between both partners. The formers can be the Ni^I cyclopentadienylnickel carbonyl dimer [CpNi(CO)]₂, the Ni^{II} nickelocene [Cp₂Ni], or the Ni^{III} nickelocenium (Cp₂Ni)(BF₄). Dithiolene sources can be 1,2-dithiete (or 1,2-dithioketone),¹⁵ [PhSb(dithiolene)],^{11,16} or the square-planar metal dithiolene complexes, [M(dithiolene)₂]ⁿ (M = Ni, Pd, and Pt; n = 0, –1) and [Pt(dithiolene)₂(dppe)] (dppe = bis(diphenylphosphino)ethane).^{12,17} Some examples of those reactions are shown in Schemes 1–3. In Scheme 1, the 2e oxidized forms of the dithiolate react with low-valent CpNi sources (Ni^I in [CpNi(CO)]₂, Ni^{II} in [Cp₂Ni]), while Scheme 2 involves the reaction of a Ni^{III} CpNi source with a protected dithiolate. Satisfactory yields were only reported in those reactions involving square-planar nickel dithiolene complexes in their anionic or neutral forms, as described in Scheme 3.

For the synthesis of the new complex [CpNi(dddt)] (dddt = 5,6-dihydro-1,4-dithiin-2,3-dithiolate) described here, we have therefore investigated different combinations of CpNi and dithiolene transfer sources. The results of these reactions are collected in Table 1 and will be discussed shortly, while details of each entry can be found in the Experimental Section. Entries 1–4 involve the thermal or photochemical activation of a 1,3-dithiole-2-one to generate, as a reactive

- (8) King, R. B. *J. Am. Chem. Soc.* **1963**, *85*, 1587.
 (9) Wharton, E. J. *Inorg. Nucl. Chem. Lett.* **1971**, *7*, 307.
 (10) Faulmann, C.; Delpech, F.; Malfant, I.; Cassoux, P. *J. Chem. Soc., Dalton Trans.* **1996**, 2261.
 (11) Fourmigué, M.; Avarvari, N. *Dalton Trans.* **2005**, 1365.
 (12) Nomura, M.; Okuyama, R.; Fujita-Takayama, C.; Kajitani, M. *Organometallics* **2005**, *24*, 5110.
 (13) Batail, P.; Boubekeur, K.; Fourmigué, M.; Gabriel, J.-C. *P. Chem. Mater.* **1998**, *10*, 3005.
 (14) Kirk, M. L.; McNaughton, R. L.; Helton, M. E. *Prog. Inorg. Chem.* **2003**, *52*, 111.

- (15) Bock, H.; Rittmeyer, P.; Stein, U. *Chem. Ber.* **1986**, *119*, 3766. (b) Krespan, C. G. *J. Am. Chem. Soc.* **1961**, *83*, 3434.
 (16) (a) Avarvari, N.; Fourmigué, M. *Inorg. Chem.* **2001**, *40*, 2570. (b) Avarvari, N.; Fourmigué, M. *Organometallics* **2003**, *22*, 2042.
 (17) Bowmaker, G. A.; Boyd, P. D. W.; Campbell, G. K. *Inorg. Chem.* **1983**, *22*, 1208.

Scheme 3



intermediate, the corresponding 1,2-dithioketone or 1,2-dithiete (shown in Scheme 1),¹⁸ but the isolated yields do not exceed 30% regardless of the nature of the CpNi source (Cp_2Ni or $[\text{CpNi}(\text{CO})]_2$). The shorter reaction time obtained with $[\text{CpNi}(\text{CO})]_2$ (entry 3) can be attributed to the concomitant thermal activation of $[\text{CpNi}(\text{CO})]_2$ for decarbonylation.¹⁹ Entries 5–7 involve the reaction of the “naked” dithiolate ddd^{2-} with either the Ni^{II} $[\text{Cp}_2\text{Ni}]$ or $[\text{CpNi}(\text{cod})]\text{BF}_4$ or the Ni^{III} $[\text{Cp}_2\text{Ni}]\text{BF}_4$ complexes, but the yields are not satisfactory (<28%). Finally, the best yields (60–85%) were obtained as described before^{11,12} with the square planar monoanionic or neutral nickel dithiolene complexes, as described in entries 8–13. Note, however, that the proper CpNi source has to be found in each case since, for example, the Ni^{II} $[\text{Cp}_2\text{Ni}]$ neutral complex does not react with $[\text{Ni}(\text{ddd})_2]^-$ (entry 9), while an 86% yield of $[\text{CpNi}(\text{ddd})]$ is obtained when using the Ni^{II} $[\text{CpNi}(\text{cod})]\text{BF}_4$ salt (entry 10), introducing the $\text{CpNi}(\text{cod})^+$ cationic species as a novel, efficient source of CpNi in these syntheses.²⁰ Similarly, the neutral, formally Ni^{IV} , $[\text{Ni}(\text{ddd})_2]$ complex²¹ was found to be inert to the Ni^{III} $[\text{Cp}_2\text{Ni}]\text{BF}_4$ (entry 12), while it reacts efficiently with the reduced $[\text{Cp}_2\text{Ni}]$ or $[\text{CpNi}(\text{CO})]_2$ neutral complexes (entries 11 and 13).

This last method was therefore used for the syntheses of the new complexes described here, $[\text{CpNi}(\text{bdt})]$ (51% yield, entry 16) and its diselenolene analogue $[\text{CpNi}(\text{bds})]$ (40% yield, entry 17). In the reaction of $[\text{Cp}_2\text{Ni}]$ with $[\text{Ni}(\text{bdt})_2]$, the oligomer of the Ni monodithiolene $[\text{Ni}(\text{bdt})]_n$ ($n = 6$) was isolated by column chromatography in a 31% yield.²² Generally, the neutral square-planar dithiolene complex has stable “dithiolate” and reactive “dithioketone” ligands, which are exhibited as $[\text{M}^{\text{II}}(\text{dithiolate})(\text{dithioketone})]$ ($\text{M} = \text{Ni}, \text{Pd}$ and Pt).²³ We assume that the coordinated dithioketone moiety reacted with a CpNi source to form the CpNi dithiolene complex, and then the remaining Ni(dithiolate) moiety is oligomerized. Some dithiolene transfer reactions using the square-planar complex $[\text{Ni}(\text{S}_2\text{C}_2\text{Ph}_2)_2]$ have been

reported;^{12,24,25,26} in this case, the corresponding oligomer $[\text{Ni}(\text{S}_2\text{C}_2\text{Ph}_2)]_n$ has been also found, including the reaction of Scheme 3b.

Similarly, the reaction of $[\text{Ni}(\text{ddd})_2]$, formulated as a dimer in a solid state,²⁷ with $[\text{Cp}_2\text{Ni}]$ produced $[\text{CpNi}(\text{ddd})]$ in a 68% yield (entry 14). Finally, the reaction of the neutral, quite insoluble $[\text{Ni}(\text{dsdt})_2]$ complex²⁸ with $[\text{Cp}_2\text{Ni}]$ in toluene gave the expected $[\text{CpNi}(\text{dsdt})]$ complex in a low yield (15%), probably together with an impurity which could not be removed but which is clearly observed on the UV–vis–NIR spectrum (see Figure 1). The CpNi dithiolene complexes $[\text{CpNi}(\text{ddd})]$, $[\text{CpNi}(\text{ddd})]$, $[\text{CpNi}(\text{dsdt})]$, $[\text{CpNi}(\text{bdt})]$, and $[\text{CpNi}(\text{bds})]$ are air-stable and soluble for normal organic solvents (dichloromethane, toluene, acetone, and THF). Their solubility decreases upon addition of *n*-hexane.

Electrochemical Data. The electrochemical behavior of CpNi dithiolene and diselenolene complexes was investigated by cyclic voltammetry (CV), and the redox potentials (vs Fc/Fc^+) are reported in Table 2, together with those of previously reported CpNi complexes for comparison. Reversible oxidation and reduction waves were found in the CVs of the five new complexes (see Supporting Information). The redox potentials of the dithiolene complexes $[\text{CpNi}(\text{ddd})]$ and $[\text{CpNi}(\text{bdt})]$ were almost similar to those of the corresponding diselenolene complexes $[\text{CpNi}(\text{ddd})]$ and $[\text{CpNi}(\text{bds})]$, respectively. This similarity was also observed between $[\text{CpNi}(\text{dmit})]$ and $[\text{CpNi}(\text{dsit})]$.¹¹ Also similar potentials are found between $[\text{CpNi}(\text{ddd})]$ and $[\text{CpNi}(\text{dsdt})]$, indicating that the redox potentials do not depend strongly on the nature of the chalcogen atoms. Note also that the evolution of the reduction potential values for the different complexes correlate well with that described for the square planar bis(dithiolene) complexes with the electrochemical series $\text{S}_2\text{C}_2\text{Me}_2 > \text{S}_2\text{C}_2\text{Ph}_2 > \text{ddd} \approx \text{bdt} > \text{dmit} > \text{mnt}$, starting with the most electron-rich dithiolate ligand. The large stability window of these metallo mono-dithiolene complexes, and its evolution with the nature of the coordinated dithiolate let us infer a good thermodynamic stability of such radical species.

Since the oxidation waves are reversible, the oxidized species of CpNi dithiolene complexes are stable on the time scale of CV measurement ($\nu = 100 \text{ mV s}^{-1}$), excluding $[\text{CpNi}(\text{mnt})]$.¹² This oxidation behavior is different from that of the 16-electron Co and Ru dithiolene complexes $[\text{CpCo}^{\text{III}}(\text{ddd})]$ and $[(\eta^6\text{-C}_6\text{R}_6)\text{Ru}^{\text{II}}(\text{S}_2\text{C}_2(\text{COOMe})_2)]$. Indeed, upon oxidation, the 15-electron cationic Co and Ru complexes immediately form dimeric species^{29,30} because the complex

- (18) (a) Kusters, W.; De Mayo, P. *J. Am. Chem. Soc.* **1974**, *96*, 3502. (b) Schroth, W.; Bahn, H.; Zschernitz, R. *Z. Chem.* **1973**, *13*, 424. (c) Schulz, R.; Schweig, A.; Hartke, K.; Koester, J. *J. Am. Chem. Soc.* **1983**, *105*, 4519.
- (19) (a) Stanghellini, P. L.; Rossetti, R.; Gambino, O.; Cetini, G. *Inorg. Chem.* **1971**, *10*, 2672. (b) Ellgen, P. C. *Inorg. Chem.* **1972**, *11*, 2279. (c) Stanghellini, P. L.; Rossetti, R.; Gambino, O.; Cetini, G. *Inorg. Chim. Acta* **1973**, *7*, 445. (d) Stanghellini, P. L.; Rossetti, R.; Gambino, O.; Cetini, G. *Inorg. Chim. Acta* **1973**, *10*, 5.
- (20) Salzer, A.; Court, T. L.; Werner, H. *J. Organomet. Chem.* **1973**, *54*, 325.
- (21) Kim, H.; Kobayashi, A.; Sasaki, Y.; Kato, R.; Kobayashi, H. *Bull. Chem. Soc. Jpn.* **1988**, *61*, 579.
- (22) This oligomer was detected by TOF-Mass (no matrix): 1192 $[\text{Ni}(\text{bdt})]_6^+$.
- (23) Schrauzer, G. N. *Acc. Chem. Res.* **1969**, *2*, 72.

- (24) Schrauzer, G. N.; Mayweg, V.; Heinrich, W. *J. Am. Chem. Soc.* **1966**, *88*, 5174.
- (25) Lim, B. S.; Donahue, J. P.; Holm, R. H. *Inorg. Chem.* **2000**, *39*, 263. (b) Goddard, C. A.; Holm, R. H. *Inorg. Chem.* **1999**, *38*, 5389.
- (26) Adams, H.; Morris, M. J.; Morris, S. A.; Motley, J. C. *J. Organomet. Chem.* **2004**, *689*, 522.
- (27) Fujiwara, H.; Ojima, E.; Kobayashi, H.; Courcet, T.; Malfant, I.; Cassoux, P. *Eur. J. Inorg. Chem.* **1998**, 1631.
- (28) Abramov, M. A.; Petrov, M. L. *Zh. Obshh. Khim.* **1996**, *66*, 1678.
- (29) Guyon, F.; Lucas, D.; Jourdain, I. V.; Fourmigué, M.; Mugnier, Y.; Cattey, H. *Organometallics* **2001**, *20*, 2421.
- (30) Nomura, M.; Fujii, M.; Fukuda, K.; Sugiyama, T.; Yokoyama, Y.; Kajitani, M. *J. Organomet. Chem.* **2005**, *690*, 1627.

Table 1. Syntheses of CpNi Dithiolene Complexes

entry	dithiolene source	CpNi source	molar ratio	solvent	condition	time (h)	product	yield (%) ^b
1	O=C(dddtt)	[Cp ₂ Ni]	1:1	toluene	reflux	24	[CpNi(dddtt)]	29
2	O=C(dddtt)	[Cp ₂ Ni]	1:1	toluene	<i>hν</i>	24	[CpNi(dddtt)]	30
3	O=C(dddtt)	[CpNi(CO)] ₂	2:1	toluene	reflux	6	[CpNi(dddtt)]	29
4	O=C(dddtt)	[CpNi(CO)] ₂	2:1	toluene	<i>hν</i>	24	[CpNi(dddtt)]	15
5	Na ₂ (dddtt)	[Cp ₂ Ni]	1:1	methanol	room temp	0.5	[CpNi(dddtt)]	6.5
6	Na ₂ (dddtt)	[Cp ₂ Ni](BF ₄)	1:1	methanol	room temp	0.5	[CpNi(dddtt)]	28
7	Na ₂ (dddtt)	[CpNi(cod)](BF ₄)	1:1	methanol	room temp	0.5	[CpNi(dddtt)]	17
8	(NBu ₄)[Ni(dddtt)] ₂	[Cp ₂ Ni](BF ₄)	1:1	methanol	reflux	2	[CpNi(dddtt)]	59
9	(NBu ₄)[Ni(dddtt)] ₂	[Cp ₂ Ni]	1:1	toluene	80 °C	2	<i>a</i>	0
10	(NBu ₄)[Ni(dddtt)] ₂	[CpNi(cod)](BF ₄)	1:1	methanol	reflux	2	[CpNi(dddtt)]	86
11	[Ni(dddtt)] ₂	[Cp ₂ Ni]	1:1	toluene	80 °C	2	[CpNi(dddtt)]	62
12	[Ni(dddtt)] ₂	[Cp ₂ Ni](BF ₄)	1:1	toluene	80 °C	2	<i>a</i>	0
13	[Ni(dddtt)] ₂	[CpNi(CO)] ₂	2:1	toluene	80 °C	2	[CpNi(dddtt)]	65
14	[Ni(dddts)] ₂	[Cp ₂ Ni]	1:1	toluene	80 °C	2	[CpNi(dddts)]	68
15	[Ni(dsdt)] ₂	[Cp ₂ Ni]	1:1	toluene	80 °C	2	[CpNi(dsdt)]	15
16	[Ni(bdt)] ₂	[Cp ₂ Ni]	1:1	toluene	80 °C	2	[CpNi(bdt)]	51
17	[Ni(bds)] ₂	[Cp ₂ Ni]	1:1	toluene	80 °C	2	[CpNi(bds)]	40

^a No reaction. ^b Isolated yield.**Table 2.** Redox Potentials of CpNi Dithiolene and Diselenolene Complexes (*E* vs Fe^{+/0})^a

	<i>E</i> _{1/2} (red) (V)	Δ <i>E</i> (mV)	Δ <i>E</i> _p (mV)	<i>E</i> _{1/2} (ox) (V)	Δ <i>E</i> (mV)	Δ <i>E</i> _p (mV)	ref
[CpNi(S ₂ C ₂ Me ₂)]	−1.38	<i>b</i>	<i>b</i>	−0.04	<i>b</i>	<i>b</i>	12
[CpNi(S ₂ C ₂ Ph ₂)]	−1.16	<i>b</i>	<i>b</i>	+0.04	<i>b</i>	<i>b</i>	12
[CpNi(dddts)]	−1.07	72	108	+0.03	74	104	this work
[CpNi(dddtt)]	−1.06	72	106	−0.02	74	106	this work
[CpNi(dsdt)]	−1.06	66	86	−0.01	68	82	this work
[CpNi(bds)]	−1.04	74	108	+0.30	74	104	this work
[CpNi(bdt)]	−1.00	68	92	+0.30	72	88	this work
[CpNi(dmit)]	−0.72	<i>b</i>	100	+0.28	<i>b</i>	100	this work
[CpNi(dsit)]	−0.74	<i>b</i>	100	+0.32	<i>b</i>	100	this work
[CpNi(mnt)]	−0.64	<i>b</i>	<i>b</i>	+0.79 ^c	<i>b</i>	<i>b</i>	12

^a *E*_{1/2} = (*E*_p + *E*_{p/2})/2, Δ*E* = |*E*_p − *E*_{p/2}|, Δ*E*_p = |*E*_{pa} − *E*_{pc}|. ^b Not available. ^c Irreversible.

alleviates an electron deficiency of the central metal. We assume that the CpNi dithiolene complexes do not dimerize upon oxidation to the cation because these oxidized complexes are formally 16-electron species.

Electron Paramagnetic Resonance. The EPR spectra of CpNi dithiolene complexes in solution in dichloromethane were measured at room temperature. They are composed of a single line whose *g* factor was measured with respect to DPPH: for [CpNi(dddtt)], *g* = 2.042; for [CpNi(dsdt)], *g* = 2.045; for [CpNi(dddts)], *g* = 2.088; for [CpNi(bdt)], *g* = 2.054; and for [CpNi(bds)], *g* = 2.095. In this work, EPR measurements were also performed for [CpNi(dmit)] (*g* = 2.044) and [CpNi(dsit)] (*g* = 2.089) for comparison purposes. The *g* values of the CpNi dithiolene complexes are similar to those of [CpNi(S₂C₂R₂)] (*g* = ~2.041–2.048; R = CF₃,³¹ Ph, COOMe, Me, and CN),¹² while the diselenolene complexes exhibit higher values because of the stronger spin–orbit

coupling with the heavier selenium atoms. Preliminary DFT calculations [UB3LYP/6-31G(d,p)]³² were performed to estimate the *g* variation caused by the replacement of a dithiolene moiety by a diselenolene moiety: passing from [CpNi(bdt)] to [CpNi(bds)] causes an increase in the calculated *g*_{av} value equal to 0.028, which is slightly smaller than the experimental value of 0.041. It is worth mentioning that the *g* values of CpNi dithiolene and diselenolene complexes are smaller than those reported for the one-electron-reduced species of the CpCo dithiolene complexes [CpCo^{II}(tfd)][−] (*g* = 2.454)³⁰ and [CpCo^{II}(mnt)][−] (*g* = ~2.5).³³ This difference in the *g* values probably reflects a difference in the spin localization: in [CpCo(dithiolene)][−] complexes, the spin is strongly localized on the central metal, while in the CpNi dithiolene complexes, it appreciably delocalizes on the dithiolene ligand (see below).¹¹ However, we could not detect the hyperfine structure resulting from ⁷⁷Se in the diselenolene complexes [CpNi(dddts)] and [CpNi(bds)] because its natural abundance is too low (7.65%). Work is in progress to prepare those selenolene complexes marked with the ⁷⁷Se isotope.

Electronic Transitions. Electronic absorption spectra were measured in a CH₂Cl₂ solution between 300 and 1500 nm

(31) Dessy, R. E.; Stary, F. E.; King, R. B.; Waldrop, M. *J. Am. Chem. Soc.* **1966**, *88*, 471.

(32) Frisch, M. J.; Trucks, G. W.; Schlegel, H. B.; Scuseria, G. E.; Robb, M. A.; Cheeseman, J. R.; Montgomery, J. A.; Vreven, T.; Kudin, K. N.; Burant, J. C.; Millam, J. M.; Iyengar, S. S.; Tomasi, J.; Barone, V.; Mennucci, B.; Cossi, M.; Scalmani, G.; Rega, N.; Petersson, G. A.; Nakatsuji, H.; Hada, M.; Ehara, M.; Toyota, K.; Fukuda, R.; Hasegawa, J.; Ishida, H.; Nakajima, T.; Honda, Y.; Kitao, O.; Nakai, H.; Klene, M.; Li, X.; Knox, J. E.; Hratchian, H. P.; Cross, J. B.; Adamo, C.; Jaramillo, J.; Gomperts, R.; Stratmann, R. E.; Yazyev, O.; Austin, A. J.; Cammi, R.; Pomelli, C.; Ochterski, J.; Ayala, P. Y.; Morokuma, K.; Voth, G. A.; Salvador, P.; Dannenberg, J. J.; Zakrzewski, V. G.; Dapprich, S.; Daniels, A. D.; Strain, M. C.; Farkas, O.; Malick, D. K.; Rabuck, A. D.; Raghavachari, K.; Foresman, J. B.; Ortiz, J. V.; Cui, Q.; Baboul, A. G.; Clifford, S.; Cioslowski, J.; Stefanov, B. B.; Liu, G.; Liashenko, A.; Piskorz, P.; Komaromi, I.; Martin, R. L.; Fox, D. J.; Keith, T.; Al-Laham, M. A.; Peng, C. Y.; Nanayakkara, A.; Challacombe, M.; Gill, P. M. W.; Johnson, B.; Chen, W.; Wong, M. W.; Gonzalez, C.; Pople, J. A. *Gaussian 03*, revision C.1; Gaussian, Inc.: Pittsburgh, PA, 2003.

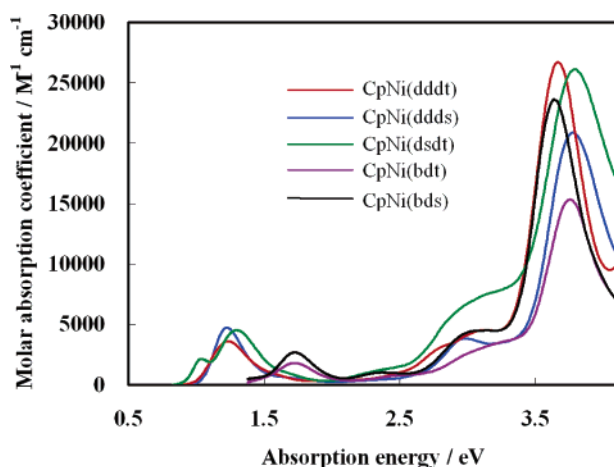
(33) McCleverty, J. A.; James, T. A.; Wharton, E. J. *Inorg. Chem.* **1969**, *8*, 1340.

Table 3. NIR Absorption Wavelengths, Associated Energies (E), and ϵ Values

	λ_{max} (nm)	E (eV)	ϵ ($\text{M}^{-1} \text{cm}^{-1}$)	ref
[CpNi(dddt)]	1012	1.225	4700	this work
[CpNi(ddds)]	1000	1.239	3600	this work
[CpNi(dsdt)]	954	1.299	5500	this work
	(1189) ^a	(1.043) ^a	(2200) ^a	
[CpNi(dmit)]	967	1.282	6000	this work
[CpNi(dsit)]	948	1.308	3200	this work
[CpNi(S ₂ C ₂ Ph ₂)]	846	1.465	2900	12
[CpNi(S ₂ C ₂ Me ₂)]	835	1.485	2600	12
[CpNi(bdt)]	722	1.717	2600	this work
[CpNi(bds)]	718	1.727	2800	this work
[CpNi(mnt)]	698	1.776	2000	12
[CpNi(S ₂ C ₂ (CO ₂ Me) ₂)]	695	1.784	1500	12

^a Values in parentheses refer to the impurity absorption (see text).

for the five new complexes, as well as for [CpNi(dmit)] and [CpNi(dsit)]. As shown in Figure 1, in addition to the UV–

**Figure 1.** UV–vis–NIR absorbance in CH₂Cl₂.

vis absorption peaks, all complexes exhibit a strong NIR (near-infrared) absorption (Table 3), observed around 1000 nm in the dddt/ddds/dsdt series, 955 nm in the dmit/dsit series, and 720 nm in the bdt/bds series, while a much lower absorption wavelength had been reported for [CpNi(mnt)] at 700 nm.¹² Such strong NIR absorptions have been known for a long time³⁴ in neutral or anionic square-planar bis-(dithiolene) complexes and were investigated for their applications as Q-switching laser dyes.³⁵ Molar extinction coefficients as high as 80 000 $\text{M}^{-1} \text{cm}^{-1}$ were even reported in neutral [M(R,R'timdt)₂] (R,R'timdt = N,N'-disubstituted imidazolidine-2,4,5-trithione).³⁶ Accordingly, the square-planar bis(dithiolene) complexes have been the subject of intense theoretical investigations in relation to their electronic structures and can be described as an essentially ligand →

Table 4. Electrochemical, Optical Properties, and Associated Energy Levels^a

	E_{ox} onset	E_{red} onset	$E_{\text{g}}^{\text{elec}}$ (eV)	$E_{\text{g}}^{\text{opt}}$ (eV)	HOMO (eV)
[CpNi(dddt)]	−0.10	−0.96	0.86	0.93	−4.70
[CpNi(dsdt)]	−0.08	−0.98	0.90		−4.72
[CpNi(ddds)]	−0.06	−0.97	0.91	0.88	−4.74
[CpNi(bdt)]	+0.20	−0.92	1.12	1.18	−5.00
[CpNi(bds)]	+0.22	−0.95	1.17	1.12	−5.02
[CpNi(dmit)]	+0.21	−0.66	0.87	1.01	−5.01
[CpNi(dsit)]	+0.25	−0.68	0.93	1.03	−5.05
[CpNi(mnt)]	+0.65	−0.55	1.20	1.30	−5.45

^a $E_{\text{g}}^{\text{elec}} = -(E_{\text{red}}\text{onset} - E_{\text{ox}}\text{onset})$, HOMO (eV) = $-[E_{\text{onset}} - E_{\text{ox}}(\text{ferrocene})] - 4.8$ with $E_{\text{ox}}\text{onset}$ in V vs Fc⁺/Fc, $E_{\text{ox}}(\text{ferrocene}) = 0$ V vs Fc⁺/Fc.

ligand one-electron promotion that possesses a small degree of LMCT character.^{37,38}

The strong NIR absorptions observed here are particularly surprising for metallo-mono(dithiolene) complexes since complexes such as (L- N_3)MoO(dithiolene) [(L- N_3) = hydrotris(3,5-dimethyl-1-pyrazolyl)borate] exhibit only very weak absorption in the NIR region with $\epsilon < 500 \text{ M}^{-1} \text{cm}^{-1}$.³⁹ The other family of mono(dithiolene) complexes investigated so far are the luminescent M(diimine)(dithiolene) ones, such as Zn(bipy)(bdt), characterized by a LLCT band in the visible region.⁴⁰ To get some, at least, qualitative insight on the electronic structures of these complexes, the nature of the NIR absorption band and its evolution with the dithiolene ligand and the optical and electrochemical data were analyzed in more detail to evaluate the HOMO/LUMO gap and associated energies in the different complexes. From the onset values of the oxidation potential and reduction potential, an electrochemical gap ($E_{\text{g}}^{\text{elec}}$) can be determined and compared with the optical gap ($E_{\text{g}}^{\text{opt}}$) determined from the onset of the low-energy NIR absorption band. We note (Table 4) that the electrochemically determined gaps are approximately the same as the optically determined ones with larger values systematically observed for the bdt/bds series, as well as for the mnt complex. The HOMO values were experimentally estimated by the onset of the oxidation potential, taking the known reference level for ferrocene, 4.8 eV below the vacuum level,⁴¹ according to the following equation: HOMO = $-[E_{\text{onset}} - E_{\text{ox}}(\text{ferrocene})] - 4.8$. As shown in Table 4, they strongly vary with the nature of the dithiolate ligand, indicating that the optical transition observed in the NIR region most probably involves energy levels with a strong dithiolene contribution. The smaller gaps being observed with the most electron-rich dithiolates

- (34) Mueller-Westerhoff, U. T.; Vance, B. In *Comprehensive Coordination Chemistry*; Wilkinson, G., Gillard, R. D., McCleverty, J. A., Eds., Pergamon: Oxford, U.K., 1987.
- (35) Mueller-Westerhoff, U. T.; Vance, B.; Yoon, D. I. *Tetrahedron* **1991**, 47, 909.
- (36) Aragoni, M. C.; Arca, M.; Demartin, F.; Devillanova, F. A.; Garau, A.; Isaia, F.; Lelj, F.; Lippolis, V.; Verani, G. *J. Am. Chem. Soc.* **1999**, 121, 7098.

- (37) Kirk, M. L.; McNaughton, R. L.; Helton, M. E. *Prog. Inorg. Chem.* **2003**, 52, 111.
- (38) Lim, B. S.; Fomitchov, D. V.; Holm, R. H. *Inorg. Chem.* **2001**, 40, 4257.
- (39) (a) Carducci, M. D.; Brown, C.; Solomon, E. I.; Enemark, J. H. *J. Am. Chem. Soc.* **1994**, 116, 11856. (b) Helton, M. E.; Gruhn, N. E.; McNaughton, R.; Kirk, M. L. *Inorg. Chem.* **2000**, 39, 2273. (c) Helton, M. E.; Kirk, M. L. *Inorg. Chem.* **1999**, 38, 4384. (d) Inscore, F. E.; McNaughton, R.; Westcott, B. L.; Helton, M. E.; Jones, R. M.; Dhawan, I. K.; Enemark, J. H.; Kirk, M. L. *Inorg. Chem.* **1999**, 38, 1401.
- (40) Cummings, S. D.; Eisenberg, R. *Prog. Inorg. Chem.* **2003**, 52, 315.
- (41) Wu, T. Y.; Sheu, R. B.; Chen, Y. *Macromolecules* **2004**, 37, 725. (b) Wu, T.-Y.; Sheu, R.-B.; Chen, Y. *Macromolecules* **2004**, 37, 725.

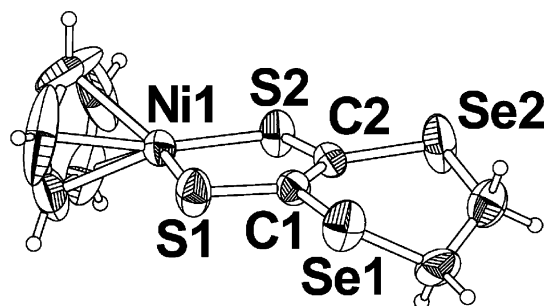


Figure 2. ORTEP drawing of [CpNi(dsdt)]. Thermal ellipsoids are drawn at the 50% probability level.

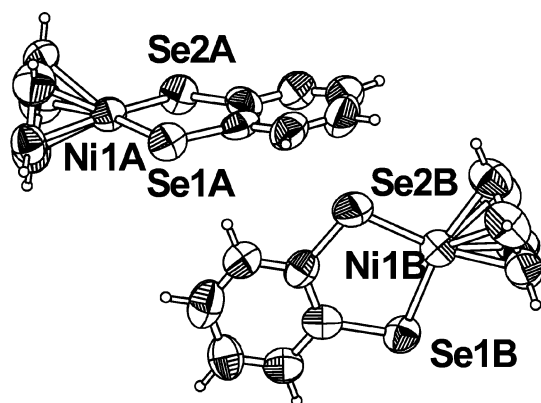


Figure 3. ORTEP drawing of the two crystallographically independent molecules in the diselenolene complex [CpNi(bds)]. Thermal ellipsoids are drawn at the 50% probability level.

allowed us to infer that even smaller ones with their associated low energy NIR absorption band could be found with very electron-rich dithiolates such as those used by Mueller-Westerhoff in square-planar nickel dithiolene complexes.^{33,34} For instance, on the basis of the evolution of the $E_{1/2}(\text{red})$ for the [CpNi(dithiolene)]⁻¹⁻⁰ process reported in Table 2, the bdt/bds complexes would be expected to exhibit smaller gaps than the dmit/dsit complexes. This is not the case, demonstrating that this NIR optical transition is not related only to the HOMO level of the anionic [CpNi(dithiolene)]⁻ complex.

Molecular Geometries. The structures of the five complexes have been determined by X-ray crystal diffraction on single crystals. [CpNi(dddt)] and its selenated analogue [CpNi(dddS)] are isostructural: they crystallize in the monoclinic system, space group $P2_1$, with four crystallographically independent molecules in the unit cell, corresponding to a 2×2 pseudoinversion center. The analogous [CpNi(dsdt)] complex is not isostructural; it crystallizes in the monoclinic system, space group $P2_1/n$, with one molecule in a general position in the unit cell (Figure 2). Similarly, [CpNi(bdt)] and its selenolene analogue [CpNi(bds)] are also isostructural; they crystallize in the monoclinic system, space group $P2_1/c$ with two crystallographically independent molecules in the unit cell (Figure 3).

Note that [CpNi(dmit)] and [CpNi(dsit)] were also found to be isostructural, demonstrating that in these [CpNi(dithiolene)] series, the S/Se substitution in the metallacycle does not substantially modify the packing of the molecules. This contrasts with the square planar bis(dithiolene) com-

plexes such as Ni(dmit)₂ⁿ, Ni(dddt)₂ⁿ, or Ni(bdt)₂ⁿ, $n = -2, -1, 0$, where the S/Se substitution to the corresponding Ni(dsit)₂ⁿ, Ni(dddS)₂ⁿ, or Ni(bds)₂ⁿ does not generally provide isostructural salts. Most probably here, the Cp ring partially hides the chalcogen atoms engaged in the nickel coordination. On the other hand, even slight modifications of the outer substituents of the dithiolene or diselenolene core do modify strongly the crystal packing, as observed here for [CpNi(dsdt)] which is not isostructural with [CpNi(dddt)] or [CpNi(dddS)].

Intramolecular bond lengths are collected in Table S1 in the Supporting Information, together with those of monoanionic square planar bis(dithiolene) or bis(selenolene) complexes for comparison purposes. The Ni–S bond lengths in [CpNi(dddt)], [CpNi(dsdt)], and [CpNi(bdt)] (~ 2.12 Å) are shorter than the Ni–Se bond lengths in [CpNi(dddS)] and [CpNi(bds)] (~ 2.25 Å). Similar tendencies have been observed in [CpNi(dmit)] versus [CpNi(dsit)],^{10,11} [Ni(dddt)₂]⁻ versus [Ni(dddS)₂]⁻,^{26,41} and [Ni(bdt)₂]⁻ versus [Ni(bds)₂]⁻ (Table 2).^{42,55} The difference between the Ni–S and Ni–Se bond lengths (~ 0.13 Å) is almost equal to that between the atomic covalent radius of sulfur and selenium. The bond lengths of the C=C double bond in the dithiolene ligands are intermediary between a C–C single and C=C double bond length, illustrating that the oxidation of the formally Ni(II) CpNi(dithiolene) complex to the neutral radical [CpNi(dithiolene)] essentially affects the dithiolene ligand. Furthermore, the C1–C2 lengths in [CpNi(bdt)] and [CpNi(bds)] (~ 1.4 Å) is slightly longer than those of the other CpNi dithiolene complexes (1.33–1.38 Å). This result is explained by not only π conjugation in a dithiolene ring but also the π conjugation of benzene ring, and this fact is also found in [Ni(bdt)₂] and [Ni(bds)₂] (C1–C2 = 1.39 Å).^{42,55} The largest

- (42) (a) McCleverty, J. A. *Prog. Inorg. Chem.* **1969**, *10*, 49. (b) Sugimori, A.; Akiyama, T.; Kajitani, M.; Sugiyama, T. *Bull. Chem. Soc. Jpn.* **1999**, *72*, 879. (c) Kajitani, M.; Hagino, G.; Tamada, M.; Fujita, T.; Sakurada, M.; Akiyama, T.; Sugimori, A. *J. Am. Chem. Soc.* **1996**, *118*, 489.
- (43) Miller, E. J.; Brill, T. B.; Rheingold, A. L.; Fultz, W. C. *J. Am. Chem. Soc.* **1983**, *105*, 7580.
- (44) Habe, S.; Yamada, T.; Nankawa, T.; Mizutani, J.; Murata, M.; Nishihara, H. *Inorg. Chem.* **2003**, *42*, 1952.
- (45) Xi, R.; Abe, M.; Suzuki, T.; Nishioka, T.; Isobe, K. *J. Organomet. Chem.* **1997**, *549*, 117.
- (46) Mashima, K.; Kaneyoshi, H.; Kaneko, S.; Mikami, A.; Tani, K.; Nakamura, A. *Organometallics* **1997**, *16*, 1016.
- (47) Hörnig, A.; Englert, U.; Kölle, U. *J. Organomet. Chem.* **1994**, *464*, C25.
- (48) Becke, A. D. *J. Chem. Phys.* **1993**, *98*, 5648.
- (49) Schaefer, A.; Horn, H.; Ahlrichs, R. *J. Chem. Phys.* **1992**, *97*, 2571. (b) Schaefer, A.; Huber, C.; Ahlrichs, R. *J. Chem. Phys.* **1994**, *100*, 5829.
- (50) Foster, J. P.; Weinhold, F. *J. Am. Chem. Soc.* **1980**, *102*, 7211.
- (51) (a) Ruiz, E.; Alemany, P.; Alvarez, S.; Cano, J. *J. Am. Chem. Soc.* **1997**, *119*, 1297. (b) Ruiz, E.; Alvarez, S.; Rodriguez-Fortea, A.; Alemany, P.; Pouillon, Y.; Massobrio, C. In *Magnetism, Molecules to Materials*; Miller, J. S., Drillon, M., Eds.; Wiley VCH: Weinheim, Germany, 2001; Vol. 2, p 227.
- (52) Baker-Hawkes, M. J.; Billig, E.; Gray, H. B. *J. Am. Chem. Soc.* **1966**, *88*, 4870.
- (53) Sandman, D. J.; Allen, G. W.; Acampora, L. A.; Stark, J. C.; Jansen, S.; Jones, M. T.; Ashwell, G. J.; Foxman, B. M. *Inorg. Chem.* **1987**, *26*, 1664.
- (54) Schultz, A. J.; Wang, H. H.; Soderholm, L. C.; Sifter, T. L.; Williams, J. M.; Bechgaard, K.; Whangbo, M.-H. *Inorg. Chem.* **1987**, *26*, 3757.
- (55) Kini, A. M.; Beno, M. A.; Williams, J. M. *J. Chem. Soc., Chem. Commun.* **1987**, 335.

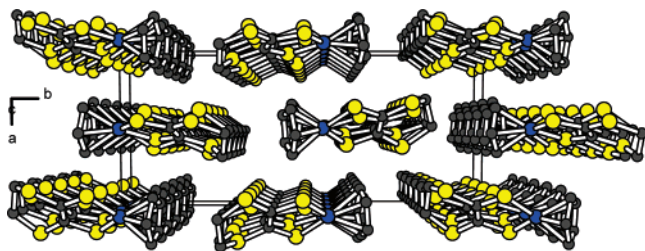


Figure 4. Projection along the *c* axis of the structure of [CpNi(dddt)].

deviations from the nickel–dithiolene and –diselenolene planes are very small (See Table S2 in Supporting Information), namely, these five-membered metallacycles are fully planar. This fact can be seen for the pseudoaromaticity of nickel–dithiolene and –diselenolene rings.⁴² In addition, the Ni–bdt (nickel–dithiolene with benzene) and the Ni–bds moieties are almost planar (largest deviations = 0.0376 Å in [CpNi(bdt)] and 0.0587 Å in [CpNi(bds)]). The dihedral angles between Cp and nickel–dithiolene (or –diselenolene) are almost a right angle. This result indicates that they are typical two-legged piano-stool geometries.

Although [CpNi(bdt)] and [CpNi(bds)] are monomers, some dimer structures have been reported in [CpCo(bdt)]₂,⁴³ [CpCo(bds)]₂,⁴⁴ [Cp*Rh(bdt)]₂ (Cp* = η^5 -pentamethyl cyclopentadienyl),⁴⁵ [$(\eta^6\text{-C}_6\text{R}_6)\text{Ru(bdt)}_2$],⁴⁶ and [Cp*Ru(bdt)]₂.⁴⁷ In these Co, Rh, and Ru complexes, the corresponding monomers have electron-poor metal centers (formal 15- or 16-electrons). As already determined above from the electrochemical behavior, we assume that the CpNi dithiolene and diselenolene complexes are not dimerized because these complexes have more electron-rich metal centers (formal 17-electrons) than those of the Co, Rh, and Ru dithiolene complexes.

Solid State Structures and Magnetic Behavior. In the solid state, the isostructural [CpNi(dddt)] and [CpNi(ddds)] radical complexes organize into columns running along the *c* axis (Figure 4), with intermolecular interactions between columns which only involve the outer sulfur atoms of the dithiine rings. The shortest S...S intermolecular contacts are observed at 3.81 and 3.86 Å, and it is anticipated that the magnetic interactions through these S...S contacts are most probably weak since the SOMO in such complexes, as already reported in [CpNi(dmit)],¹¹ is essentially localized on the NiS₂C₂ or NiSe₂C₂ metallacycles.

On the other hand, within the columns running along *c* (Figure 5), short intermolecular S...S, Se...S, and Se...Se contacts involving chalcogen atoms of the metallacycles are now identified, giving rise in both complexes to spin chains running along *c*, with S...S contacts of 3.75 and 4.05 Å in [CpNi(dddt)] and Se...Se contacts of 3.84 and 3.96 Å in [CpNi(ddds)]. The situation is notably different in [CpNi(dsdt)] where similar but uniform spin chains are found to run along the *a* axis (Figure 6).

The temperature dependence of the magnetic susceptibility (Figure 7) of [CpNi(dddt)], [CpNi(ddds)], and [CpNi(dsdt)] reflects these different structural organizations. It exhibits indeed a Curie–Weiss type behavior in the high-temperature regime with $\theta_{\text{dddt}} = -46$ K, $\theta_{\text{ddds}} = -36$ K, and $\theta_{\text{dsdt}} = -58$

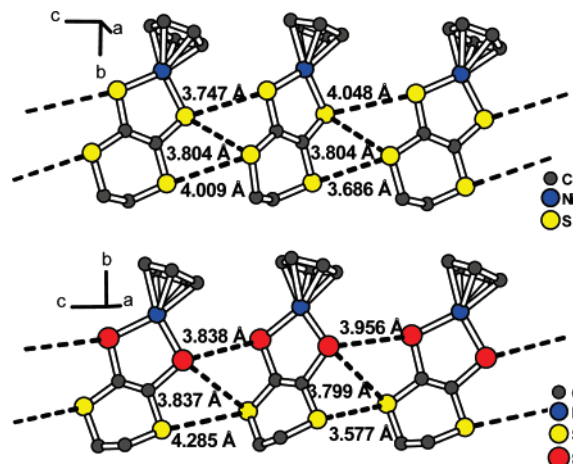


Figure 5. Alternating chains of (top) [CpNi(dddt)] and (bottom) [CpNi(ddds)] radical complexes running along *c*.

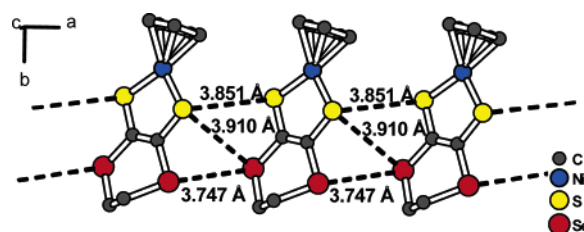


Figure 6. Detail of the uniform chain of [CpNi(dsdt)] radical complexes running along *a*.

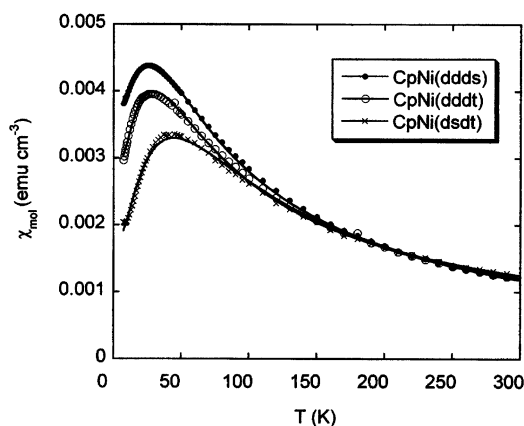


Figure 7. Temperature dependence of the magnetic susceptibility of [CpNi(dddt)] (O), [CpNi(ddds)] (●), and [CpNi(dsdt)] (×). Solid lines are fits to alternated chain models (see text).

K, demonstrating the presence of strong antiferromagnetic interactions between the radical moieties, with stronger interactions in the dsdt complex. A susceptibility maximum is observed in all complexes, at 27 K in [CpNi(dddt)], 25 K in [CpNi(ddds)], and at a higher temperature (45 K), as anticipated from the θ_{dsdt} value, in [CpNi(dsdt)]. No field dependence of the susceptibility below these temperature maxima was observed, ruling out the possibility of an ordered antiferromagnetic ground state in the three compounds.

On the basis of the structure descriptions given above for the two isostructural [CpNi(dddt)] and [CpNi(ddds)] complexes, an alternated chain model with J and αJ , $0 < \alpha < 1$, was used to fit the data, yielding close values: $J_{\text{dddt}}/k = -65$ K (45 cm⁻¹), $J_{\text{ddds}}/k = -66$ K (46 cm⁻¹), $\alpha_{\text{dddt}} = \alpha_{\text{ddds}} = 0.7$. On the other hand, a Heisenberg uniform chain model

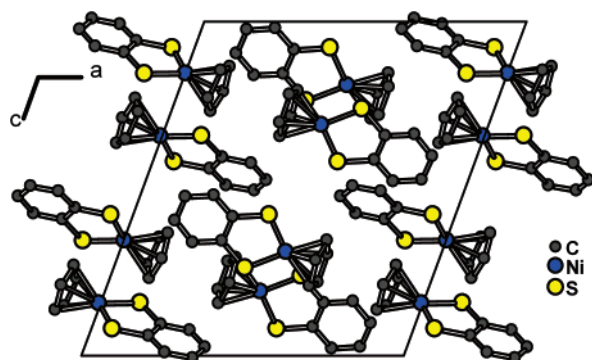


Figure 8. Projection view along the b axis of the unit cell of [CpNi(bdt)].

can be considered to fit the magnetic data of [CpNi(dsdt)]. However, such a model could not fit satisfactorily the experimental data, and a slight alternation had to be introduced in the chain model ($\alpha = 0.9$) to take into account the activated part of the susceptibility below $T(\chi_{\max})$, yielding a J/k value of -77 K (53 cm $^{-1}$). This failure to fit the magnetic susceptibility down to low temperatures with the Bonner–Fisher model probably reflects a tendency of the uniform chains identified in the room-temperature X-ray crystal structure of [CpNi(dsdt)] to undergo a weak dimerization upon cooling which opens a gap in the energy dispersion of the chain. Indeed, upon dimerization, an alternated spin chain is formed, whose magnetic behavior is characterized by a singlet ground state and an activated susceptibility in the low-temperature region.

As mentioned above, [CpNi(bdt)] and [CpNi(bds)] are isostructural and crystallize with two crystallographically independent molecules, A and B in the following. In the solid state, the radical molecules organize perpendicular to each other (Figure 8), and short intermolecular chalcogen...chalcogen contacts can hardly be identified as the shortest intermolecular S...S distances are 4.42 Å between the A molecules and 4.75 Å between the B molecules in [CpNi(bdt)], and the shortest Se...Se intermolecular distances are found at 4.25 Å between the A molecules and 4.65 Å between the B molecules in [CpNi(bds)].

It is therefore anticipated that the radical species are essentially independent from each other and that the temperature dependence of their magnetic susceptibility should follow a Curie or Curie–Weiss law. As shown in Figure 9, this is absolutely not the case: a broad susceptibility maximum around room temperature is observed together with a Curie contribution at the lowest temperatures. This behavior testifies for the presence of strong antiferromagnetic interactions, which cannot be attributed here to chalcogen...chalcogen or chalcogen...nickel interactions. A closer inspection of the crystal structures of [CpNi(bdt)] and [CpNi(bds)] reveals an original feature which has not been seen before in these series: an almost face-to-face arrangement of the Cp rings of molecules A and B (Figure 10) with C...C intermolecular distances as short as 3.32 and 3.37 Å in [CpNi(bdt)] and [CpNi(bds)], while the angles between the Cp mean planes are 4.46 and 4.17° in [CpNi(bdt)] and [CpNi(bds)], respectively.

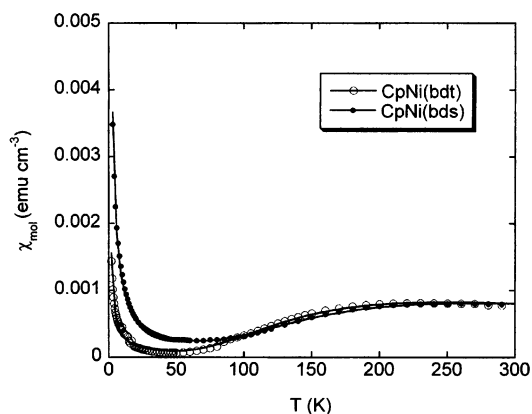


Figure 9. Temperature dependence of the magnetic susceptibility of [CpNi(bdt)] (○) and [CpNi(bds)] (●). Solid lines are fits to the Bleaney–Bower singlet–triplet model with a Curie tail at the lowest temperatures (see text).

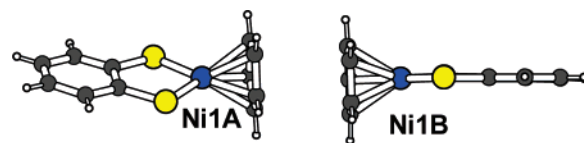


Figure 10. Detail of the dyadic association between A and B molecules in [CpNi(bdt)] showing the Cp...Cp face-to-face interaction.

At this stage, we can tentatively conclude that the strong antiferromagnetic interaction observed in those complexes can be attributed to this original Cp...Cp overlap. Taking this solid-state organization into account, we performed a fit of the susceptibility data with a singlet–triplet model, together with a contribution, observable at low temperatures, of a Curie-type susceptibility (Curie tail) attributable to paramagnetic defaults. The best fits afforded J/k values of $-402(4)$ (279 cm $^{-1}$) and $-451(6)$ K (313 cm $^{-1}$), together with Curie contribution of 0.8 and 2.6% $S = 1/2$ species for the [CpNi(bdt)] and [CpNi(bds)] complexes, respectively. To strengthen this hypothesis, quantum calculations were performed on the [CpNi(bdt)] complex to obtain the shape of its SOMO, as well as the distribution of the spin density. The calculations were performed with the Gaussian03 code³¹ with the hybrid B3LYP functional.⁴⁸ We have employed a triple- ζ all-electron Gaussian basis set for the nickel atoms and a double- ζ basis set for the other elements proposed by Schaefer et al.⁴⁹ As shown in Figure 11, the SOMO is largely distributed on the dithiolate ligand and the nickel atom, as already observed for the SOMO of [CpNi(dmit)].¹¹

It is therefore expected that the antiferromagnetic interactions would be dominated by interactions between the dithiolate ligands when present. However, as shown in Table 5, Mülliken and NBO⁵⁰ analysis of the spin distribution show that 40 – 42% of the spin density is delocalized on the nickel atom, 31 – 32% on the two chalcogen atoms, and a far from negligible 21% on the cyclopentadienyl ring. These results confirm that, in the absence of any intermolecular S...S or Ni...S interactions, the Cp...Cp overlap observed in the X-ray crystal structure of [CpNi(bdt)] can indeed justify the strong antiferromagnetic interaction experimentally deduced from the temperature dependence of the magnetic susceptibility.

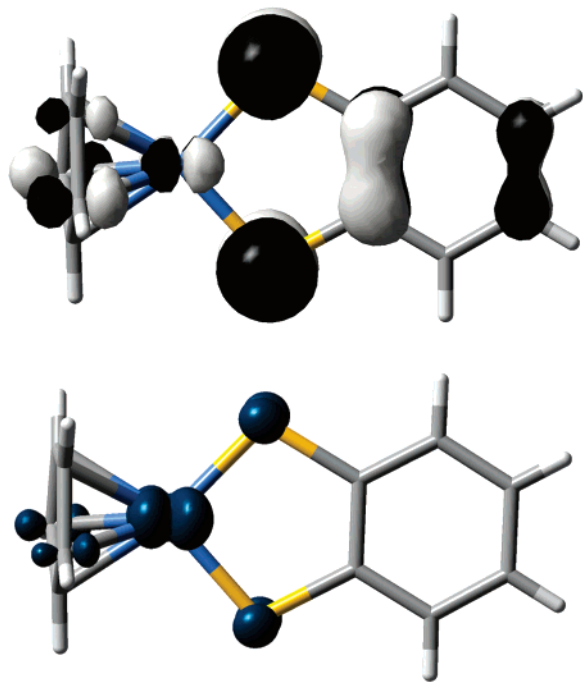


Figure 11. (top) Calculated SOMO of [CpNi(bdt)] (DFT UB3LYP/triple- ζ all-electron basis set for the iron atoms and a double- ζ basis set for the other elements). (bottom) Spin density distribution in [CpNi(bdt)]. The isodensity surface represented corresponds to a value of $0.01 \text{ e}^-/\text{bohr}$.³

Table 5. Calculated Spin Density (Mulliken and NBO analysis) in [CpNi(bdt)] and [CpNi(ddd)] Complexes

	Ni	S1 + S2	Cp	others
[CpNi(ddd)] Mulliken	0.28	0.40	0.12	0.20
[CpNi(ddd)] NBO	0.28	0.42	0.12	0.19
[CpNi(bdt)] Mulliken	0.42	0.32	0.21	0.05
[CpNi(bdt)] NBO	0.42	0.31	0.21	0.06

Similar calculations performed on the [CpNi(ddd)] complex shows also a large delocalization of the SOMO, and as shown in Figure 12, the spin density is largely delocalized on the whole metallacycle with only 12% left on the Cp ring. These observations justify a posteriori the assumption made above that the strongest intermolecular interactions in [CpNi(ddd)] were essentially attributable to S \cdots S contacts. They also give us some insight about the probable differences between the two classes of complexes which were identified above. Indeed, while both [CpNi(bdt)] and [CpNi(ddd)] appeared to fit nicely in the well-established electrochemical series known for square-planar bis(dithiolene) complexes with $\text{S}_2\text{C}_2\text{Me}_2 > \text{S}_2\text{C}_2\text{Ph}_2 > \text{ddd} \approx \text{bdt} > \text{dmit} > \text{mnt}$, the much lower energy absorption band (1000 nm) observed only in [CpNi(ddd)] and [CpNi(dmit)] identify those two complexes as peculiar in the series and demonstrate unambiguously that the energy of the NIR absorption band is not uniquely correlated to differences in the HOMO energy level. The above calculations tend to show that the presence of thioalkyl or selenoalkyl substituents on the dithiolene core induces a strong delocalization of the spin density on the whole metallacycle, while in the other complexes, a sizable spin density is observed on the cyclopentadienyl ring.

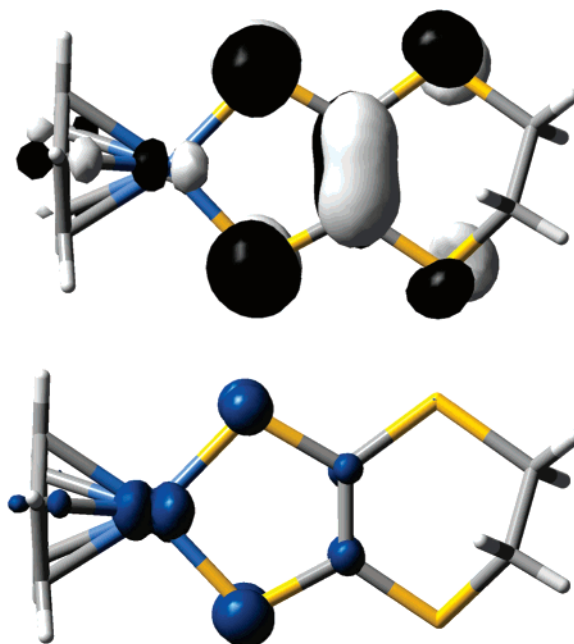


Figure 12. (top) Calculated SOMO of [CpNi(ddd)] (DFT UB3LYP/triple- ζ all-electron basis set for the iron atoms and a double- ζ basis set for the other elements). (bottom) Spin density distribution in [CpNi(ddd)]. The isodensity surface represented corresponds to a value of $0.01 \text{ e}^-/\text{bohr}$.³

Conclusion

The investigation of novel synthetic procedures for the preparation of these [CpNi(dt)] series has shown that the partially oxidized dithiolene complexes $[\text{Ni}(\text{dt})_2]^{1-}$ react not only with the air-sensitive Ni^{III} $[\text{Cp}_2\text{Ni}]\text{BF}_4$ species, as observed earlier,^{11,12} but also, in good yields, with the air stable Ni^{II} [CpNi(cod)] BF_4 complex, providing a very efficient route particularly adapted to electron-poor dithiolate ligands available as $[\text{Ni}(\text{dt})_2]^{1-}$ anions. On the other hand, the oxidized $[\text{Ni}(\text{dt})_2]^0$ complexes were shown to react not only with the Ni^{II} $[\text{Cp}_2\text{Ni}]$ complex¹² but also with the Ni^{I} $[\text{CpNi}(\text{CO})]_2$ dimer with comparable and good yields. A strong NIR absorption band is observed in all complexes, but it is at a particularly low energy (1000 nm) in the dddt and dmit complexes (and selenated analogues) when compared with $\text{S}_2\text{C}_2\text{Me}_2$, $\text{S}_2\text{C}_2\text{Ph}_2$, bdt, or mnt complexes, where it is observed between 750 and 800 nm. Finally, an original intermolecular Cp \cdots Cp σ overlap has been identified in the solid state structure of [CpNi(bdt)] and [CpNi(bds)] as the only possible pathway for a strong antiferromagnetic interaction, which most probably finds its origin in a sizable spin density distribution of the cyclopentadienyl ring, a very original feature in organometallic radical complexes. Theoretical investigations are currently underway to (i) determine the origin of the NIR absorption of these complexes, particularly in [CpNi(dmit)] and [CpNi(ddd)], and (ii) to quantitatively evaluate the magnetic coupling constants.⁵¹

Experimental Section

General Remarks. All reactions were carried out under an argon atmosphere by means of standard Schlenk techniques. All solvents for chemical reactions were dried and distilled by Na benzophenone (for toluene) or CaH₂ (for methanol) before use. The square-planar

Table 6. Crystallographic Data of CpNi Dithiolene and Diselenolene Complexes

	CpNi(dddt)	CpNi(ddds)	CpNi(dsdt)	CpNi(bdt)	CpNi(bds)
formula	C ₉ H ₉ NiS ₄	C ₉ H ₉ NiS ₂ Se ₂	C ₉ H ₉ NiS ₂ Se ₂	C ₁₁ H ₉ NiS ₂	C ₁₁ H ₉ NiSe ₂
fw	304.11	397.91	397.91	264.01	357.81
cryst color	black	black	black	black	brown
cryst size (mm)	0.40 × 0.30 × 0.08	0.39 × 0.24 × 0.06	0.54 × 0.21 × 0.01	0.30 × 0.30 × 0.04	0.54 × 0.24 × 0.04
cryst system	monoclinic	monoclinic	monoclinic	monoclinic	monoclinic
space group	<i>P</i> 2 ₁	<i>P</i> 2 ₁	<i>P</i> 2 ₁ / <i>n</i>	<i>P</i> 2 ₁ / <i>c</i>	<i>P</i> 2 ₁ / <i>c</i>
<i>a</i> (Å)	9.1045(8)	9.2009(8)	6.2605(5)	15.1132(10)	15.5585(15)
<i>b</i> (Å)	20.766(2)	20.963(2)	21.146(2)	9.3294(7)	9.4950(7)
<i>c</i> (Å)	12.3642(11)	12.6630(11)	9.2234(7)	16.3831(10)	16.5769(16)
β (deg)	105.119(10)	105.827(10)	106.276(9)	110.596(7)	112.131(11)
<i>V</i> (Å ³)	2256.8(4)	2349.8(4)	1172.11(18)	2162.3(3)	2268.5(4)
<i>T</i> (K)	293(2)	293(2)	293(2)	293(2)	293(2)
<i>Z</i>	8	8	4	8	8
<i>D</i> _{calcd} (g cm ⁻³)	1.790	2.250	2.255	1.622	2.095
μ (mm ⁻¹)	2.413	8.158	8.178	2.133	8.084
total reflns	17 675	18 689	9139	20 329	16 861
unique reflns (<i>R</i> _{int})	8598 (0.0475)	8585 (0.0621)	2148 (0.0907)	4161 (0.0727)	4341 (0.1018)
unique reflns (<i>I</i> > 2σ(<i>I</i>))	6362	5867	1457	2096	1987
<i>R</i> ₁ , <i>R</i> ₂ (<i>I</i> > 2σ(<i>I</i>)) ^a	0.0394, 0.0954	0.0365, 0.0796	0.0619, 0.1528	0.0340, 0.0788	0.0648, 0.1434
<i>R</i> ₁ , <i>R</i> ₂ (all data) ^a	0.0566, 0.1027	0.0681, 0.0935	0.0862, 0.1761	0.0909, 0.1003	0.1354, 0.1739
GOF	0.803	0.945	0.945	0.703	0.840

$$^a R_1 = \sum ||F_o| - |F_c|| / \sum |F_o|; wR_2 = [\sum w(F_o^2 - F_c^2)^2 / \sum wF_o^4]^{1/2}.$$

nickel dithiolene complexes, [Ni(dddt)₂],²¹ [Ni(ddds)₂],²⁶ [Ni(dsdt)₂],²⁷ [Ni(bdt)₂],⁵² [Ni(bds)₂],⁵³ and (NBu₄)[Ni(dddt)₂],⁵⁴ were synthesized by literature methods. O=C(dddt),⁵⁵ [Cp₂Ni](BF₄),⁵⁶ and [CpNi(cod)](BF₄)²⁰ were prepared by literature methods. [Cp₂Ni] and [CpNi(CO)]₂ were obtained from STREM Chemicals and Aldrich Chemicals, respectively. Silica gel (Silica gel 60) was obtained from MERCK, Ltd. The TOF-mass spectrum was recorded on a Bruker Daltonics MALDI-TOF BIFLEX III mass spectrometer. UV-vis and NIR spectra were recorded on Hitachi Model UV-2500PC and PERKIN ELMER Model Lambda 19 UV/VIS/NIR spectrometers, respectively. Elemental analyses were performed by the "Service d'Analyse du CNRS" at Gif/Yvette, France. UV irradiation for a photoreaction was performed with a high-pressure Hg lamp (Applied Photophysics, Ltd).

Reactions of [Cp₂Ni] or [CpNi(CO)]₂ with the Neutral Square-Planar Nickel Dithiolene and Diselenolene Complexes. A toluene solution (50 mL) of [Cp₂Ni] (38 mg, 0.2 mmol) and the square-planar dithiolene complexes [Ni(dithiolene)₂] (dithiolene = dddt, ddds, bdt, and bds; 0.2 mmol) was reacted at 80 °C for 2 h. After the solvent was removed under reduced pressure, the residue was separated by a column chromatography (silica gel, dichloromethane/*n*-hexane = 1:1 (v/v)). The product was further purified by recrystallization (*n*-hexane/dichloromethane). The corresponding CpNi dithiolene complexes, [CpNi(dddt)] (black crystal, 62% yield), [CpNi(ddds)] (black crystal, 68% yield), [CpNi(bdt)] (black crystal, 51% yield), and [CpNi(bds)] (brown crystal, 40% yield), were obtained. The reaction of [CpNi(CO)]₂ (30 mg, 0.1 mol) with [Ni(dddt)₂] (84 mg, 0.2 mmol) was performed in the manner noted above.

Reaction of [Cp₂Ni](BF₄) or [CpNi(cod)](BF₄) with (NBu₄)-[Ni(dddt)₂]. [Cp₂Ni](BF₄) (55 mg, 0.2 mmol) and (NBu₄)[Ni(dddt)₂] (132 mg, 0.2 mmol) in methanol (50 mL) was reacted under reflux. An initial green solution was rapidly changed to a black cloudy solution. After the mixture reacted under reflux for 2 h, the solution color changed to greenish brown. The solvent was removed under reduced pressure, and the reaction mixture was separated by a column chromatography (silica gel, dichloromethane/*n*-hexane = 1:1 (v/v)). The product was further purified by recrystallization (*n*-

hexane/dichloromethane). [CpNi(dddt)] was obtained in a 59% yield. [CpNi(cod)](BF₄) (64 mg, 0.2 mmol) reacted with (NBu₄)-[Ni(dddt)₂] (132 mg, 0.2 mmol) to give [CpNi(dddt)] in an 86% yield.

Thermal Reactions of [Cp₂Ni] or [CpNi(CO)]₂ with O=C(dddt). A solution of [Cp₂Ni] (94 mg, 0.5 mmol) and O=C(dddt) (104 mg, 0.5 mmol) was reacted in refluxing toluene for 24 h. After the reaction, silica gel was added to the reaction mixture, and then, the remaining [Cp₂Ni] was rapidly oxidized and adsorbed onto the silica gel. The mixture was separated by column chromatography (silica gel, dichloromethane/*n*-hexane = 1:1 (v/v)). The black solid of [CpNi(dddt)] was obtained in a 29% yield. The thermal reaction of [CpNi(CO)]₂ (76 mg, 0.25 mmol) with O=C(dddt) (104 mg, 0.5 mmol) was also performed, and [CpNi(dddt)] was isolated in a 29% yield.

Photoreactions of [Cp₂Ni] or [CpNi(CO)]₂ with O=C(dddt). A toluene solution (300 mL) of [Cp₂Ni] (57 mg, 0.3 mmol, *c* = 1.0 × 10⁻³ mol dm⁻³) and [O=C(dddt)] (63 mg, 0.3 mmol, *c* = 1.0 × 10⁻³ mol dm⁻³) was reacted for 24 h by using UV irradiation from a high-pressure Hg lamp (400 W). After the reaction, a black precipitate was filtered off, and the filtrate was evaporated under reduced pressure. The residue was separated by a column chromatography (silica gel, dichloromethane/*n*-hexane = 1:1 (v/v)). The black solid of [CpNi(dddt)] was obtained in a 30% yield. The photoreaction of [CpNi(CO)]₂ (46 mg, 0.15 mmol, *c* = 5.0 × 10⁻⁴ mol dm⁻³) with O=C(dddt) (63 mg, 0.3 mmol, *c* = 1.0 × 10⁻³ mol dm⁻³) for 24 h also gave [CpNi(dddt)] in a 15% yield.

Reaction of [Cp₂Ni], [Cp₂Ni](BF₄) or [CpNi(cod)](BF₄) with Na₂(dddt). O=C(dddt) (63 mg, 0.3 mmol) was treated with 2 equiv of sodium methoxide in a methanol solution (20 mL). The colorless solution turned yellow after 1 h at room temperature. In this moment, the naked 1,2-dithiolate of disodium salt (Na₂(dddt)) is generated. When [Cp₂Ni](BF₄) (83 mg, 0.3 mmol) was added into this solution, the yellow solution immediately changed to brown. The reaction mixture was further stirred at room temperature for 0.5 h. When air was blown into the solution, the brown solution changed to greenish-brown. After the solvent was removed under reduced pressure without heating, the residue was separated by a column chromatography (silica gel, dichloromethane/*n*-hexane =

(56) Miller, J. S.; Calabrese, J. C.; Rommelmann, H.; Chittipeddi, S. R.; Zhang, J. H.; Reiff, W. M.; Epstein, A. J. *J. Am. Chem. Soc.* **1987**, *109*, 769.

1:1 (v/v)). [CpNi(ddd)] was obtained in a 28% yield. [Cp₂Ni] or [CpNi(cod)](BF₄) reacted with Na₂(ddd) in the same condition noted above.

[CpNi(ddd)]. TOF-Mass (MALDI, 19 kV): m/z 303 (M⁺), 275 (M⁺ – (CH₂)₂). UV–vis–NIR (CH₂Cl₂, λ_{\max} (ε)): 1012 (4700), 417 (4600), 329 (24 000), 270 nm (14 000). Anal. Calcd for C₉H₉NiS₄: C, 35.54; H, 2.98; S, 42.17. Found: C, 35.64; H, 3.17; N, 42.12.

[CpNi(ddd)]. TOF-Mass (MALDI, 19 kV): m/z 399 (M⁺(⁸⁰Se)), 371 (M⁺(⁸⁰Se) – (CH₂)₂). UV–vis–NIR (CH₂Cl₂, λ_{\max} (ε)): 1000 (3600), 395 (1800), 339 (23 000), 270 nm (15 000). Anal. Calcd for C₉H₉NiS₂Se₂: C, 27.17; H, 2.28; S, 16.12. Found: C, 27.15; H, 2.35; S, 16.32.

[CpNi(dsdt)]. TOF-Mass (MALDI, 19 kV): m/z 399 (M⁺(⁸⁰Se)), 371 (M⁺(⁸⁰Se) – (CH₂)₂). UV–vis–NIR (CH₂Cl₂, λ_{\max} (ε)): 1189 (2200), 954 (5500), 327 nm (26 000). Anal. Calcd for C₉H₉NiS₂Se₂: C, 27.17; H, 2.28; S, 16.12. Found: C, 27.33; H, 2.46; S, 16.22.

[CpNi(bdt)]. TOF-Mass (MALDI, 19 kV): m/z 263 (M⁺). UV–vis (CH₂Cl₂, λ_{\max} (ε)): 722 (2600), 330 nm (15 000). Anal. Calcd for C₁₁H₉NiS₂: C, 50.04; H, 3.44; S, 24.29. Found: C, 50.17; H, 3.56; S, 24.42.

[CpNi(bds)]. TOF-Mass (MALDI, 19 kV): m/z 359 (M⁺). UV–vis (CH₂Cl₂, λ_{\max} (ε)): 718 (2800), 393 (4700), 341 nm (24 000). Anal. Calcd for C₁₁H₉NiS₂: C, 36.92; H, 2.54. Found: C, 37.06; H, 2.65.

X-ray Diffraction Studies. The single crystals of CpNi dithiolenes complexes were obtained by recrystallization from the dichloromethane solutions and vapor diffusion of *n*-hexane into those solutions. Crystals were mounted on the top of a thin glass fiber. Data were collected on a Stoe Imaging Plate diffraction system (IPDS) with graphite-monochromated Mo K α radiation (λ = 0.71073 Å) at room temperature. Structures were solved by direct methods (SHELXS-97) and refined (SHELXL-97) by full-matrix least-squares methods. Absorption corrections were applied. Hydrogen atoms were introduced at calculated positions (riding model), included in structure factor calculations, and these were not refined. Crystallographic data of complexes are summarized in Table 6.

CV Measurements. All electrochemical measurements were performed under an argon atmosphere. Solvents for electrochemical measurements were dried with 4 Å molecular sieves before use. A platinum wire served as a counter electrode, and the Ag/AgCl reference electrode was corrected for junction potentials by being referenced internally to the ferrocene/ferrocenium (Fc/Fc⁺) couple. A stationary platinum disk (1.6 mm in diameter) was used as a

working electrode. The Model CV-50W instrument from BAS Co. was used for cyclic voltammetry (CV) measurements. CVs were measured in 1.0 mmol dm^{−3} dichloromethane solutions of complexes containing 0.1 mol dm^{−3} tetrabutylammonium hexafluorophosphate (NBu₄PF₆) at 25 °C.

EPR Measurements. The preparations of sample solutions for EPR measurements were carried out in a drybox; 1.0 mmol dm^{−3} dichloromethane solutions of complexes were prepared, except for the solution of [CpNi(dsdt)], which was prepared in toluene solution. The EPR spectra were recorded on a Bruker ESP 300 spectrometer (X-band), except for that of [CpNi(dsdt)], which was investigated on a Bruker EMX EPR spectrometer (X-band).

Magnetic Susceptibility Measurements. Magnetic susceptibility measurements were performed on a Quantum Design MPMS-2 SQUID magnetometer operating on the range of 2–300 K at 5000 G with polycrystalline samples of [CpNi(ddd)] (17.88 mg), [CpNi(ddd)] (9.53 mg), [CpNi(dsdt)] (8.14 mg), [CpNi(bdt)] (19.73 mg), and [CpNi(bds)] (58.4 mg). Gelatin capsules were used with a magnetization contribution of $-2.37 \times 10^{-6} + (2.2 \times 10^{-6}/(T + 2))$ emu G^{−1} which was used for correction of the experimental magnetization. Molar susceptibilities were then corrected for Pascal diamagnetism. Fits to the alternated chain model are based on the following expression (eq 1) of the spin Hamiltonian for an alternated chain, $-A_{2i-1} - (J) - A_{2i} - (\alpha J) - A_{2i+1}$, while the susceptibility of the [CpNi(bdt)] and [CpNi(bds)] complexes was fitted with eq 2 where x is the fraction of $S = 1/2$ magnetic defaults

$$H = -J \sum [S_{A_{2i}} S_{A_{2i-1}} + \alpha S_{A_{2i}} S_{A_{2i+1}}] \quad (1)$$

$$\chi = (1 - x) \frac{Ng^2\beta^2}{kT[3 + \exp(-J/kT)]} + x \frac{Ng^2\beta^2}{2kT} \quad (2)$$

Acknowledgment. We thank Prof. Masatsugu Kajitani (Sophia University) for help with the CV measurements and Dr Ph. Blanchard (CNRS-University of Angers) for help with the NIR measurements. T.C. thanks the Ministerio de Educación y Ciencia (Spain) for a PhD grant.

Supporting Information Available: CIF files giving crystallographic data for [CpNi(ddd)], [CpNi(ddd)], [CpNi(dsdt)], [CpNi(bdt)], and [CpNi(bds)], tables of bond distances and angles, and a figure for the cyclic voltammetry. This material is available free of charge via the Internet at <http://pubs.acs.org>.

IC0608546